Climate Dynamics (2006) 27: 677–694
DOI 10.1007/s00382-006-0153-5

B. G. Hunt

The Medieval Warm Period, the Little Ice Age and simulated climatic variability

Received: 19 April 2005 / Accepted: 24 March 2006 / Published online: 11 May 2006

Abstract The CSIRO Mark 2 coupled global climatic model has been used to generate a 10,000-year simulation for 'present' climatic conditions. The model output has been analysed to identify sustained climatic fluctuations, such as those attributed to the Medieval Warm Period (MWP) and the Little Ice Age (LIA). Since no external forcing was permitted during the model run all such fluctuations are attributed to naturally occurring climatic variability associated with the nonlinear processes inherent in the climatic system. Comparison of simulated climatic time series for different geographical locations highlighted the lack of synchronicity between these series. The model was found to be able to simulate climatic extremes for selected observations for century timescales, as well as identifying the associated spatial characteristics. Other examples of time series simulated by the model for the USA and eastern Russia had similar characteristics to those attributed to the MWP and the LIA, but smaller amplitudes, and clearly defined spatial patterns. A search for the frequency of occurrence of specified surface temperature anomalies, defined via duration and mean value, revealed that these were primarily confined to polar regions and northern latitudes of Europe, Asia and North America. Over the majority of the oceans and southern hemisphere such climatic fluctuations could not be sustained, for reasons explained in the paper. Similarly, sustained sea–ice anomalies were mainly confined to the northern hemisphere. An examination of mechanisms associated with the sustained climatic fluctuations failed to identify a role for the North Atlantic Oscillation, the El Niño-Southern Oscillation or the Pacific Decadal Oscillation. It was therefore concluded that these fluctuations were generated by stochastic processes intrinsic to the nonlinear climatic system. While a number of characteristics of the MWP and the LIA could have been partially caused by natural processes within the climatic system, the inability of the model to reproduce the observed hemispheric mean temperature anomalies associated with these events indicates that external forcing must have been involved. Essentially the unforced climatic system is unable to sustain the generation of long-term climatic anomalies.

B. G. Hunt
CSIRO Marine and Atmospheric Research, PMB1,
Aspendale, VIC 3195, Australia
E-mail: barrie.hunt@csiro.au

1 Introduction

The Medieval Warm Period (MWP) is generally considered to be an episode of above average temperatures for the years 950–1200 AD, while the Little Ice Age (LIA) was an episode of below average temperatures from 1550 to 1850 AD (Brazdil et al. 2005). However, there is no universal agreement as regards the precise dates of these events, and they were not episodes of continuous above or below average temperatures. In fact, controversy continues to exist over the reality of both the MWP and LIA. For example, Hughes and Diaz (1994) question whether the MWP ever really occurred, while, on the other hand, Grove (1998) has documented the LIA in considerable detail. Bradley et al. (2003) have also discussed this issue. Recently, Jones and Mann (2004) seriously question the basis for the existence of both the MWP and the LIA.

In IPCC (2001, Chapter 2) there is a lengthy discussion of the climatic characteristics associated with the MWP and LIA, which again queries the basis for these events. The principal concerns listed are the lack of temporal correspondence between climatic variability in different regions, regional variability itself, the modest amplitude of the hemispheric mean temperature anomalies, and the sparseness and derivative nature of the observations. Jones and Mann (2004) are even more critical, and question the relevance of much of the colloquial evidence for these events, such as the existence in England of vineyards during the MWP and frost fairs

during the LIA. These issues primarily arise because of uncertainties in the climatic reconstructions.

On the other hand, there are many observational studies documenting climatic perturbations, primarily temperature, that advocate the occurrence of these events (see, for example, Petersen 1994; Villalba 1994; Keigwin 1996; Broecker 2001; Cronin et al. 2003 and Cook et al. 2004). A particularly comprehensive review of historical climatic fluctuations over Europe has been presented recently by Brazdil et al. (2005).

This issue is not just an academic disagreement, as it has entered into the discussion of the credibility of the attribution of the current warming to the greenhouse effect. Mann et al. (1999), based largely on proxy data, have derived a northern hemispheric temperature time series from 1000 AD to the present. This time series has a 'hockey stick' shape with the curve of the stick representing the global warming over the past few decades, while the shaft of the stick represents the fairly stationary time series of hemispheric temperature anomalies back to 1000 AD. The crucial issue is that no MWP is identified by the time series, thus justifying the probability that 1998 was the warmest year, and the 1990s the warmest decade, of the past millennium in the northern hemisphere (Mann et al. 1999). The significance of this statement is that this implies natural climatic variability cannot account for the present observed global warming, as concluded, for example, by Davies and Hunt (1994), from model simulations.

Natural, or internal, climatic variability is defined here to be that which occurs solely due to internal interactions of the climatic system, without any external forcing whatsoever. This internal forcing is a consequence of the complex physical processes which occur, together with nonlinear interactions, that can generate stochastic outcomes.

A major, currently unresolved, issue regarding past climatic fluctuations is the individual role played by the various possible forcing agents: natural variability, volcanic eruptions, solar perturbations and varying greenhouse gas concentrations.

In the case of greenhouse gases, specifically CO_2, its concentration has increased from about 280 ppm prior to about 1850 to over 370 ppm currently (IPCC 2001). The present global warming is widely accepted as being attributable to this recent increase in CO_2, implying that the lower CO_2 concentrations over the previous millennium were associated with a generally cooler climate (see, for example, Rind et al. (2004)). There is also general agreement that large volcanic eruptions have a transient impact on climate for 2–3 years following an eruption. Differing estimates of the radiative impact of eruptions and their occurrences currently exist (see Crowley and Kim 1999; Zorita et al. 2005).

The role of solar perturbations is, however, much more controversial. There have been many attempts to estimate the impact of solar perturbations on climate over the past millennium. For example, Beer et al. (2000) used a regression analysis and estimated that possibly 40% of climatic variation was attributable to solar influences, with 50% to greenhouse gases and 10–20% to internal variability. Using an energy balance model Crowley and Kim (1999) concluded that about 1/3 of low frequency climatic variability was attributable to solar influences, with the remainder due to greenhouse gases and internal variability. Numerous climatic model simulations have been made, see below, that include solar perturbations over past centuries, and these typically indicate a major contribution of such perturbations to climatic variability.

However, substantial questions have been raised concerning the reality of the impact of solar fluctuations on climate. For example, Foukal et al. (2004) have queried the observational evidence used to claim that solar forcing has varied over the past few centuries. While not dismissing such a possibility they demonstrate that supporting evidence to date is inadequate because of the derivative basis of past estimates of solar variability. More importantly, based on an analysis of the physical processes occurring in the sun, Lean et al. (2002) have questioned whether the proxies used to estimate radiative forcing actually imply fluctuations in solar forcing. In addition, Damon and Laut (2004) have strongly challenged some specific claims that solar forcing is the cause of the present observed global warming.

Perhaps most critically, is the recent observational analysis of Turney et al. (2005). They used trees in Ulster to obtain a common-dated radiocarbon calibration curve (to derive solar activity) and reconstruct temperature values for the past 9,000 years. Such common-dating has not been available previously. They concluded that at centennial to millennial timescales North Atlantic climatic variability was not forced by solar fluctuations. This outcome raises major questions concerning the numerous claims that have been made concerning the substantial role of solar forcing of climate.

The final contributor to past climatic perturbations, namely internal climatic variability, is generally considered to have an influence, albeit of a subsidiary nature (Rind and Overpeck 1993; Collins et al. 2002) A more substantive role has been advocated by Hunt (1998), in disagreement with the conclusions of Bell et al. (2003).

Given the spatial and temporal limitations of observations, and the problems of deriving quantitative climatic values from proxy data, a natural recourse is to use global climatic models to investigate past climatic fluctuations. Jones and Mann (2004) provide a brief discussion of this issue.

Jones et al. (1998), in a study primarily concerned with the quality of proxy data, compared such data with two model outputs. They used principal component and cross spectra analyses and noted substantial differences between the ability of the two models to represent spatial structures. Collins et al. (2002) compared two estimates of proxy observations with a 1,200-year simulation with a coupled model. They examined time series for specific regions and estimated the variance and power spectra of

the proxy and simulated datasets. Some underestimation of variance by the model was noted, particularly with the second analysis of the proxy measurements. Shindell et al. (2003) in a simulation involving forcing by volcanic eruptions and solar variability concluded that long-term regional climatic changes seem to have been dominated by solar influences. The impact of volcanic eruptions on surface temperature has been assessed in a comprehensive empirical and modelling study by Shindell et al. (2004). They were able to simulate many observed features. The primary climatic response for winter conditions was for a warming over Eurasia and eastern USA and cooling over northern Africa and the Middle East. The volcanic impact lasted about 2 years, with the generated temperature anomalies ranging up to a maximum of ± 1.5 K. Because of cancellation between opposite signed temperature anomalies the hemispheric or global mean change would have been quite small. Zorita et al. (2004, 2005) have also produced a simulation for the last 500 years using a coupled model forced by fluctuations of solar variability, volcanic activity and varying greenhouse gas concentrations. They obtained time series of temperature anomalies that substantially exceeded most reconstructions and remarkably uniform spatial distributions of temperature anomalies over most of the globe.

A simulation by von Storch et al. (2004) resulted in large hemispheric mean negative temperature anomalies (> -0.4 K) between 1400 and 1900 AD, with peak values above 1.0 K in 1780. These outcomes indicate the difficulty in specifying the role and magnitude of external forcing, as well as limitations associated with climatic models.

Other simulations using solar and volcanic external forcings have reproduced the reconstructed climatic variability over the past millennium to varying degrees, and are thus strong advocates for the necessity of such forcings in order to explain the observations. For example, Goosse et al. (2005) using a 25-member ensemble mean obtained general agreement with observations, but for the more representative case of individual simulations considerable differences were apparent between these simulations, implying differences also with the observations. Of particular interest to the present paper was their identification of the important role of internal climatic variability in the evolution of their climatic time series. Other simulations (Waple et al. 2002; Shindell et al. 2004) exhibited regional scale positive and negative surface temperature anomalies, as did Goosse et al. (2005) for individual members of their ensemble. In contrast, Zorita et al. (2004) show a ubiquitous cooling over the northern hemisphere for a mean over 1680–1710 AD presumably indicative of excessive external forcing as suggested by their Fig. 2. In a very comprehensive simulation, involving a range of external forcings, Rind et al. (2004) reported on the extensive, induced climatic fluctuations they obtained. In their ensemble mean results they also reported almost total global cooling for their experiments for the period 1651–1700 AD, again indicative of excessive external forcing. Perhaps their most interesting finding was that historical greenhouse gas concentrations may have contributed to cooling during the Maunder Minimum (1645–1715 AD). In this regard the recent book by Ruddiman (2005) is of relevance as it offers an interesting speculation to account for (small) greenhouse gas fluctuations over the historical past that could have contributed to climatic anomalies. Bertrand et al. (2002), using a rather simple model, conducted a range of sensitivity experiments involving solar, volcanic and anthropogenic external forcings. Again, their experiments highlight the problems of specifying external forcings, but serve to emphasise the potential importance of such forcing as an explanation of climatic variability over the last millennium.

The current paper is largely motivated by the critique of Jones and Mann (2004) concerning the reality of the MWP and LIA. It should be noted, however, that the present simulation was made to examine a large range of climatic issues, and was not specifically concerned with the MWP and LIA. The 10,000-year simulation does not represent a progression of climate over the Holocene, but an extended simulation of 'present' climatic variability. This permits a large range of climatic events to be sampled in the individual millennia of the simulation, particularly extreme events where, for example, 1 in 10,000 year events have been identified.

With the availability of this multi-millennial simulation it seems worthwhile to revisit the issues considered in Hunt (1998), as a much more comprehensive analysis is now possible. Specifically, insight will be sought into the temporal and spatial extent of regional climatic anomalies, and their magnitudes, attributable to naturally occurring climatic variability. Thus, the aim of the paper is to determine the extent to which internally generated climatic anomalies may have contributed to the concept of the MWP and LIA. In particular, can plausible outcomes be achieved without resorting to external forcing.

The definition of naturally occurring climatic variability used here needs to be contrasted with that of Jones and Mann (2004) who state "that solar and volcanic forcing have likely played the dominant roles among the potential natural causes of climate variability". Given the difficulty of separating out the individual contributions of the various possible external forcing agents from natural variability in observations, there seems to be a tendency amongst observationalists to attribute any observed climatic perturbation to external influences [see for example Hodell et al. (2001) versus the outcome of Hunt and Elliott (2005)]. Also, in a recent discussion of climatic changes, Esper et al. (2005) categorise natural forcing mechanisms as those associated with solar variability, volcanic eruptions and greenhouse gases, but not internal variability of the climatic system. This reluctance amongst observationalists to acknowledge a contribution from internal climatic variability has resulted in an undue emphasis on the role of external

forcings. It is hoped that the present paper may partially rectify this bias.

Importantly, this paper does not mandate the existence or absence of the MWP and the LIA in the historical record. What it attempts to show is that a number of the climatic fluctuations usually associated with these events can be found in the present simulation. Whether these results strengthen the case for the MWP and LIA is left to the reader to decide.

The degree to which the present model can simulate observed climatic features has been documented in a range of papers, see for example Gordon and O'Farrell (1997); Hunt (2001, 2004); Hunt and Elliott (2002), 2003, 2005). Independent analyses of the present model's performance have been made as part of extensive model intercomparisons by AchutaRao and Sperber (2000) and Covey et al. (2000). The model performed very capably in these assessments.

2 Model description and experimental details

The CSIRO Mark 2 coupled global climatic model was used to generate the data sets used in this paper. The model consists of atmospheric, oceanic, biospheric and sea–ice components, as described by Gordon and O'Farrell (1997). The horizontal resolution of the model is based on the R21 spectral formulation, implying gridboxes spaced at 5.625° longitudinally and 3.25° latitudinally, giving a total of 3,584 gridboxes per vertical level distributed over the global surface.

The atmospheric and oceanic components interact via radiative and heat fluxes and dynamical processes at the oceanic surface for each model timestep of 20 min. The widely used flux correction technique (Sausen et al. 1988) was applied to couple these two components. These corrections vary monthly, but being invariant from year-to-year do not influence interannual variability and thus the simulated climate.

The atmospheric model has nine vertical levels, diurnal and seasonal variability, a mass flux convection scheme, semi-Lagrangian water vapour transport, gravity wave drag and a cloud parameterization based on relative humidity. The oceanic model is based on the Geophysical Fluid Dynamics Laboratory code, with temperature and salinity grid points corresponding to those used in the atmospheric model. The oceanic model has twenty-one vertical levels and realistic bottom topography. An eddy-induced advection scheme was implemented thus enabling the background diffusivity to be set to zero. Wind forcing of the upper three oceanic levels is crudely represented by setting a minimum lower limit to the vertical diffusivity, see Hirst et al. (2000) for further details.

The biospheric scheme has a number of different soil and plant types, with the latter's properties varying on a monthly timescale. A rather simple two-layer soil moisture formulation is used.

Thermal processes determine the growth and decay of sea–ice, while dynamical processes can cause thinning or compaction of the ice. The sea–ice can also be transported by oceanic currents or wind forcing.

The present simulation was initiated from a previous 1,000-year simulation of the model; hence all climatic variables were fully developed. The model was run out for 10,000 years for present climatic conditions, using an atmospheric CO_2 concentration of 330 ppm. No external forcings such as solar perturbations, volcanic forcing or changes in greenhouse gas concentrations were permitted during the model run. Thus, all climatic perturbations obtained are attributable to naturally occurring climatic variability generated solely by processes internal to the simulated climatic system.

All results presented here have been restricted to a single millennium of the simulation, years 9,001–10,000. This is an arbitrary choice; results for other millennia are very similar except for outlier events specific to a given millennium. The choice of a single millennium for analysis is appropriate given that the MWP and LIA were effectively limited to the last millennium.

3 Temporal and spatial relationships

In Fig. 1 100-year simulated time series of annual mean surface temperatures are compared for six different model gridboxes. All results are for the northern hemisphere for reasons that will become apparent later. These time series are essentially unremarkable and reveal anomalies of, at most, ± 2 K. Similar variabilities are obtained in millennial length reconstructed time series documented by Serre-Bachet (1994) and Diaz and Pulwarty (1994). In effect, the model is simulating annual mean surface temperature variability comparable to these particular observations, which do not exhibit any indication of the existence of the MWP and the LIA. Temporal correlations between the various time series in Fig. 1 for the years 9,100–10,000 were all less than 0.2, with the majority below 0.1. This lack of synchronicity has also been noted in observations by Graumlich (1993); Hughes and Diaz (1994); Jones et al. (1998) and Jones and Mann (2004), and discussed in relation to model simulations by Goosse et al. (2005). Nevertheless, there are numerous other reconstructed time series, see the several examples presented by Jones and Mann (2004), that exhibit a range of variability, some of which support the occurrence of the MWP and LIA. The complexity of the situation is well illustrated by reconstructed time series presented by Jones et al. (1998) that exhibit markedly different variability across Europe. For example, some of these time series indicated extended cold episodes in the 1500 and 1600 s, whilst others are almost time-invariant, see also Collins et al. (2002). Briffa et al. (2004) have produced spatial plots of warm season temperature anomalies for the northern hemisphere for selected years with the largest positive and

negative anomalies. These results are rather restricted in their spatial coverage, being largely confined to high latitude land regions. Distinct differences are apparent in the overall sign of the anomaly patterns for the warm and cold years, but, importantly, both positive and negative temperature anomalies occur in all years. A similar outcome is also shown in Mann et al. (1998).

Examination of individual, exceptionally warm and cold years in the simulation, not shown, revealed comparable situations for annual mean conditions to those of Briffa et al. (2004). Less consistency and more spatial variability were found when individual months were examined. Briffa et al. (2004) also show a number of anomalously warm years in the period usually associated with the LIA, reinforcing the point that this was not an epoch with conditions continuously colder than normal.

Jones and Mann (2004) present time series of reconstructed temperature anomalies from 200 to 2000 AD that have both the northern and southern hemispheres with negative values for almost the whole of this period. Such consistent negative anomalies, which have a magnitude of only about −0.4 K, would require some external forcing agent. They cannot be explained by natural climatic variability, see Hunt (2004). A possible, credible agent, is simply lower CO_2 atmospheric concentrations, as Rind et al. (2004) found lower CO_2 values quite effective in producing an overall cooling.

The present model used a CO_2 concentration of 330 ppm. If the simulation had been run with a value of 280 ppm for a notional period from 1000 to 1880 AD and then increased steadily to 330 ppm, a systematic cooling would have been obtained for these earlier years. The negative temperature anomalies would also have been enhanced if they were calculated with respect to a 1960–1990 mean rather that the 1,000-year mean. Inclusion of large volcanic eruptions would also have generated multi-year cooling impacts and so help to explain some of the particularly anomalous outcomes, see for example Wagner and Zorita (2005).

Time series (not shown) for annual rainfall for the same points as used in Fig. 1, revealed considerably more interannual variability but even lower correlations.

Historical time series of sustained regional temperature anomalies have been given by Grove (1998); Biondi et al. (1999) and Luterbacher et al. (2004) amongst others. For example, Luterbacher et al. (2004) provide European mean temperature anomalies for 1500–2003, while Biondi et al. (1999) give July temperature anomalies for a small region in Idaho, USA for the last millennium. A specific test was therefore undertaken to see whether the simulation could replicate the basic characteristics of these observations.

Figure 2a illustrates July surface temperature anomalies normalised (by the 9,001–10,000 year standard deviation) for a model gridbox in Idaho, while Fig. 2b illustrates annual mean simulated surface temperature anomalies for Europe. Both time series have a 10-point running mean curve superimposed to emphasise longer-term variability. The different formats of the time series in Fig. 2 correspond to the formats used by Biondi et al. (1999) for Idaho and Luterbacher et al. (2004) for Europe.

The normalised temperature anomalies for Idaho range over ± 3 SD, somewhat larger than those reported by Biondi et al. (1999). Hence the simulated natural climatic variability for this location can attain, and exceed, the reconstructed values. The timesmoothed values in Fig. 2a show a higher frequency variability than the reconstructions, but this appears to be attributable to the heavier timesmoothing used by Biondi et al. For example, timesmoothed results from corals presented by Felis and Patzold (2004) reveal higher frequency variability in better agreement with Fig. 2. The simulation has more extremes exceeding ± 2 SD, but where such extremes occur in the reconstructions they persist for a number of years. The reconstructions reveal three extreme cold episodes centred on about 1300, 1450 and 1610 AD, with the latter attributed by Biondi et al. (1999) to a volcanic eruption. These extremes sustained values of − 2 SD over decadal periods. The simulation appears to be unable to sustain such extremes. This is probably the most important distinction between the simulation and reconstructions.

In the case of Europe, Fig. 2b, the simulation has fewer extreme negative anomalies than reconstructions, but noticeably more positive anomalies. Sustained cold events are a feature of the reconstructions, while, again, the simulation has rather more decadal variability. The timesmoothed curve of the reconstructions is below average from 1500 to 1900, while the simulation, Fig. 2b, clearly shows alternating warm and cold, multi-decadal periods. Certainly, the positive anomalies between 9,500 and 9,600 years, and overall cold anomalies between 9,100 and 9,500 years in Fig. 2b could be considered supportive of the MWP and LIA respectively, but do not have sufficiently long durations with clearly defined positive and negative anomalies.

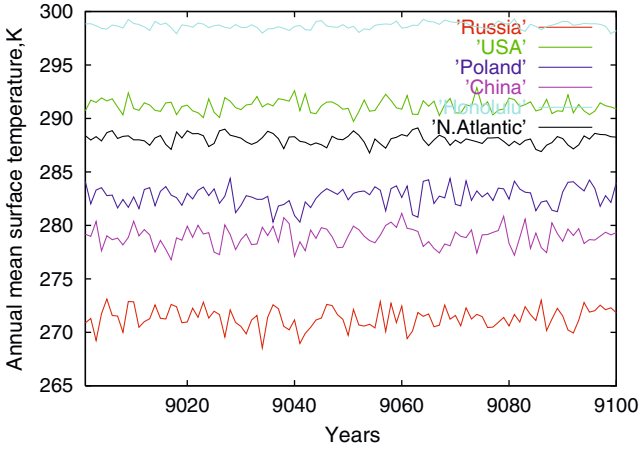

Fig. 1 Time series of annual mean surface temperature for years 9,001–9,100 of the 10,000-year simulation. All results are for individual model gridboxes. Russia (60°N, 60°E); USA (30°N, 100°W); Poland (50°N, 20°E); China (30°N, 100°E); Honolulu (20°N, 160°W) and North Atlantic (45°N, 30°W)

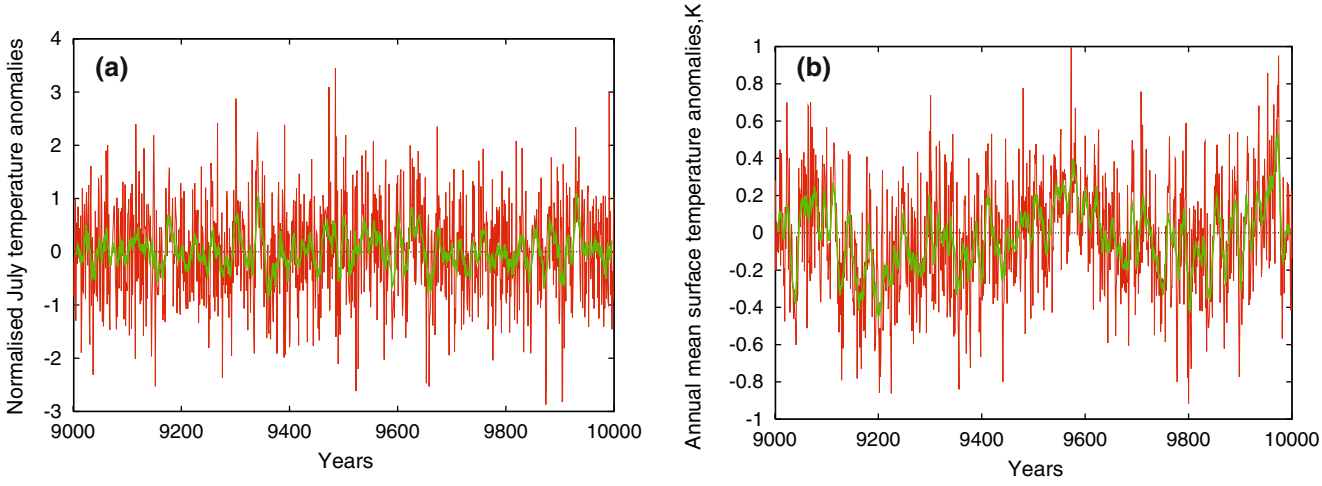

Fig. 2 Time series of surface temperature anomalies for a gridbox in Idaho, USA (43°N, 114°W) and the European region (35–70°N, 25–40°E) are shown in panels **a** and **b**, respectively for years 9,001–10,000 of the simulation. The Idaho time series are normalised July values. The European time series are annual mean values. In each case the heavy *green lines* in the panels are 10-point running means

Luterbacher et al. (2004) also present a composite of the surface temperature anomalies over Europe for the ten coldest winters in the last 500 years. This showed negative temperature anomalies over all of continental Europe, with the largest anomalies (−7 K) over northwest Russia. Positive anomalies were found over Iceland and most of Turkey. A similar composite of the ten coldest winters (defined here as January, February and March) derived from the time series in Fig. 2b was made for the simulation. The resulting global distribution is shown in Fig. 3b. The outcome over continental Europe was remarkably similar to that of Luterbacher et al. (2004). Noticeable positive temperature anomalies also occur over North America and the Bering Strait, but with reduced amplitudes. No temperature anomalies outside the range ± 1 K were found over the oceans. Interestingly, while Fig. 3b is for northern hemisphere winter conditions, and thus southern hemisphere summer, the latter hemisphere is basically devoid of any noticeable temperature anomalies.

When the analysis for Fig. 3b was repeated for another millennium a very similar outcome was obtained. This suggests that this European temperature anomaly pattern is a consistent climatological feature (although only 10 years of the millennium were used to produce the figure), see below for further discussion of this European feature.

A similar analysis was undertaken for the ten warmest Julys for the Idaho time series of Fig. 2a. The resulting global composite surface temperature anomalies are shown in Fig. 3a. A large regional response with temperature anomalies above 1 K can be seen within the USA, but these positive anomalies are considerably smaller than the negative anomalies over Europe in Fig. 3b. Again the response over the oceans and southern hemisphere land areas was minimal, apart from the Antarctic region.

The asymmetric hemispheric response in Fig. 3 is discussed below.

The important outcome from these results is that simulated naturally occurring climatic variability can produce substantial regional temperature anomalies similar to historical observations. In particular, the results in Fig. 3b agree with observations over Europe for the past 500 years when the LIA supposedly occurred, but they do not suggest a hemispheric mean response such as reported by Jones and Mann (2004) and simulated by Goosse et al. (2005).

While the time series in Fig. 1 mainly exhibit, at most, decadal variability, longer-term variability did occur in the simulation. Such variability appears to be characteristic of observations associated with the MWP and LIA and some examples from the 10,000-year simulation are shown in Fig. 4. These examples are for individual gridboxes located within Russia and the USA, as these countries appear to have the most noticeable responses, see Fig. 3.

In Fig 4a, b simulated annual mean surface temperature anomalies are illustrated, while in Fig. 4c, d simulated monthly mean anomalies are displayed for somewhat shorter periods for clarity. The results for the USA, Fig. 4a, show an approximately 20-year period of above average temperatures, with individual years attaining anomalies above 1.5 K. A similar period of below average temperatures for Russia is shown in Fig. 4b, with anomalies reaching −2 K. The corresponding monthly surface temperature anomalies in Fig. 4c, d reveal much larger anomalies, ranging up to ± 8 K, and that the respective warm and cold conditions prevailed for much of the year. The duration of these episodes is similar to some reconstructed time series (D'Arrigo et al. 2001; Biondi et al. 1999; Briffa et al. 2004), but there are also many examples where much longer duration episodes prevailed (Briffa et al. 2004; Biondi et al. 1999; Jones and Mann 2004).

Although the time series in Fig. 4 are far too short to represent either the MWP or the LIA, they serve to indicate that sustained periods of above or below aver-

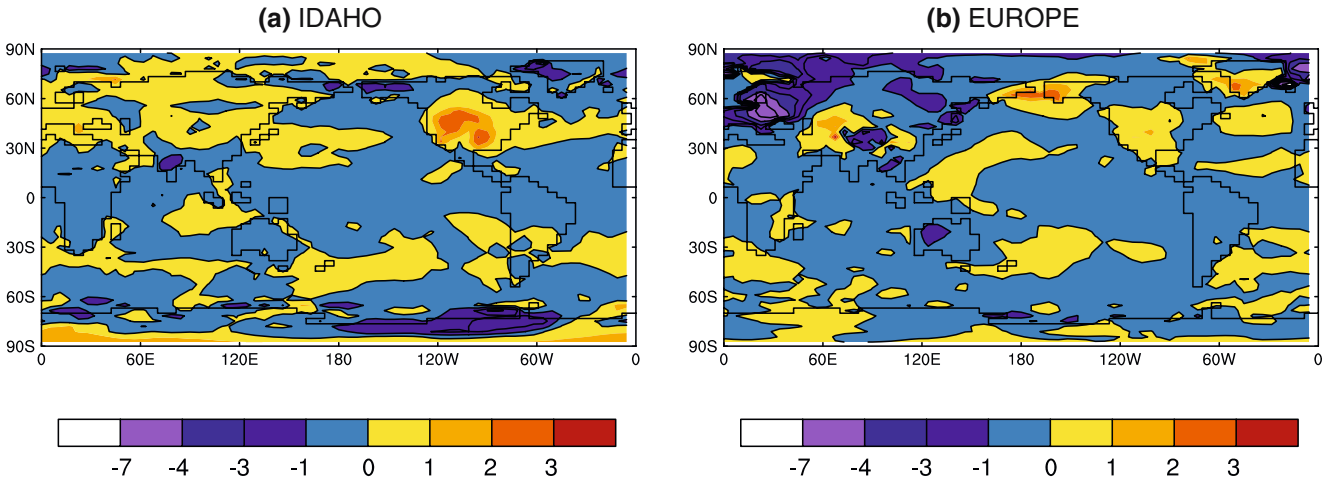

Fig. 3 Global distributions of surface temperature anomalies for the ten most extreme years in the period 9,001–10,000 years of the simulation, as depicted in Fig. 2. Panel **a** is for the ten warmest Julys for the Idaho gridbox, panel **b** for the ten coldest winters in the European region. The *colour bars* are in K

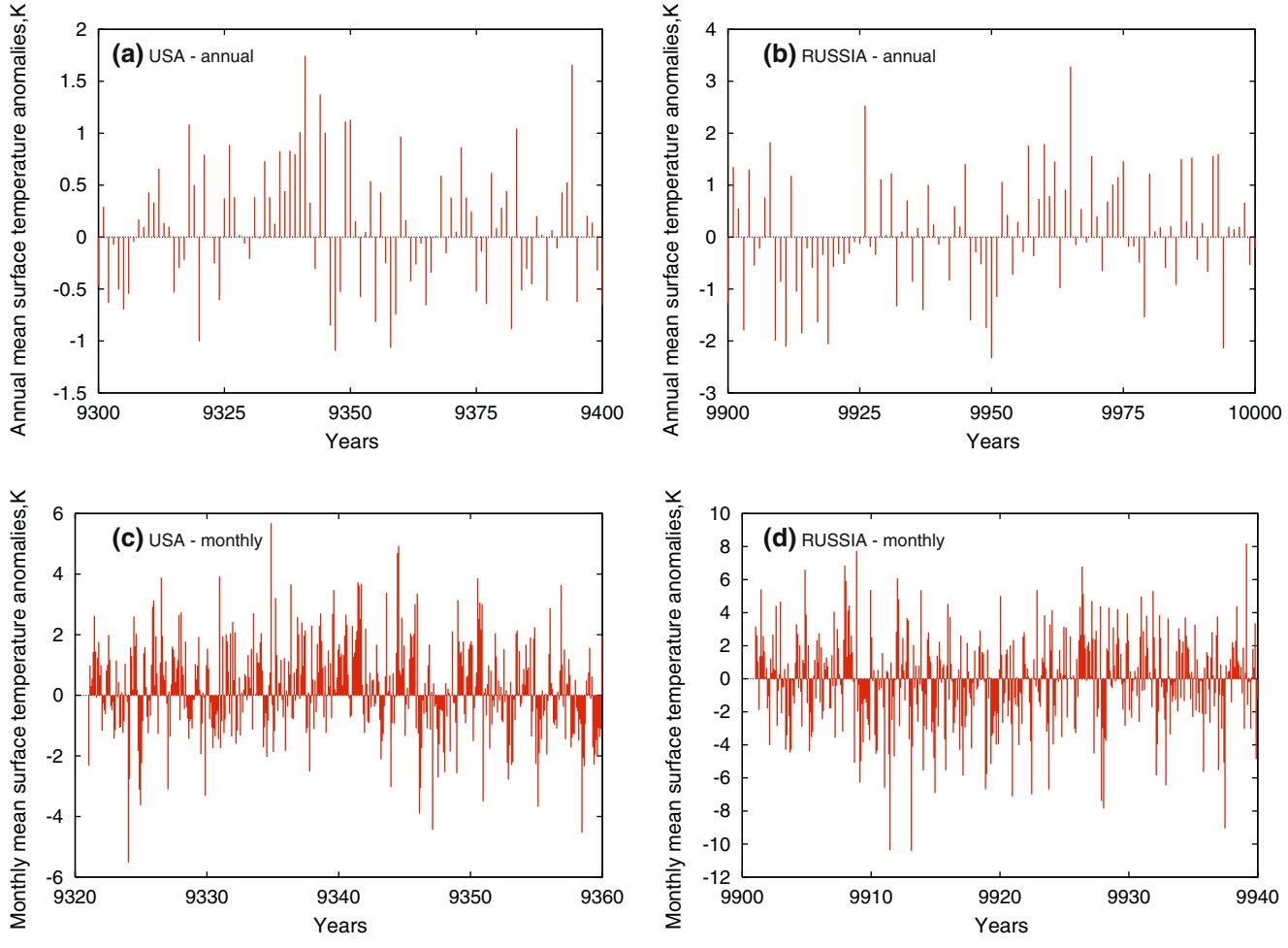

Fig. 4 Time series of annual mean and monthly mean surface temperature anomalies are given in the *upper* and *lower* panels, respectively. The *left hand* panels illustrate an extended period of positive anomalies for a gridbox in the USA (30°N, 100°W), and the *right hand* panels negative anomalies for the gridbox in Russia (60°N, 60°E).

age temperatures of considerable magnitude can be generated by naturally occurring climatic variability alone. Presumably, it is the occurrence of a number of such periods, not necessarily all with such large anomalies as shown in Fig. 4, coupled with years having normal interannual variability, that might have given credence to the concepts of the MWP and the LIA. It is the occurrence of sequences of years with extreme climatic anomalies that tends to categorise the characteristics for longer periods embracing such extremes. That the simulation can sustain longer periods with more modest temperature anomalies of a given sign is illustrated below.

Time averages of global distributions of simulated annual mean surface temperatures, appropriate to the time series shown in Fig. 4, are illustrated in Fig. 5. A modest warming over the period is shown for the USA in Fig. 5a, concentrated on the southeast of the continent, and similar in magnitude to the observations of Briffa et al. (2004). A concurrent warming of similar magnitude occurred over Scandinavia, while some below average temperatures can be seen over Asia and Canada. Thus a hemispheric-wide cooling was clearly not established for this period. Much larger negative anomalies can be seen in conjunction with the locations of sea–ice in both hemispheres. Again, as noted in relation to Fig. 3, only minor temperature anomalies are to be found over southern hemispheric land and most of the oceans. A substantial region, with negative temperature anomalies, extending from western Russia and covering most of northern Asia, Alaska and Canada, can be seen in Fig. 5b, similar to results for the 1600s in Briffa et al. (2004). Mean temperature anomalies of about −1 K were attained. The regionality of the warming region in Fig. 5a is especially marked, and supports the comments made by Jones and Mann (2004) concerning the apparent lack of global or hemispheric synchronicity in past climatic variations. Rather less spatial variability was obtained in a similar time-averaged anomaly plot for the MWP in the forced simulation of Goosse et al. (2005). This presumably explains their hemispheric mean anomalies.

Interestingly, Zorita et al. (2004) reproduced a similar outcome over western Europe to that in Fig. 5b with a *forced* simulation. Importantly, they also give an observational estimate of temperature anomalies over western Europe, averaged for the 35-year period 1675–1710 AD, which was again remarkably similar to Fig. 5b, having positive anomalies over Scandinavia and negative anomalies over much of western Europe. The principal discrepancy with Fig. 5b was that the maximum negative anomalies were simulated too far eastwards. This *particular* outcome indicates that external forcing is not always necessary to reproduce *sustained*, observed regional temperature anomalies.

While Fig. 5 provides two specific examples of long duration events, it is also useful to obtain a global perspective of the frequency of occurrence of such events. This typically cannot be derived from observations. A search of all ten millennia of the simulation was made for events of a specified duration, which also had a specified mean surface temperature anomaly over that duration for individual gridboxes. Figure 6 provides an example of the outcomes. This figure shows the frequency of occurrence, at individual model gridboxes, of 100-year duration events for which the mean temperature anomalies were ± 0.2 K, and 30-year duration events where the mean anomalies were ± 0.5 K. The search routine was designed to prevent multiple counts within a given sequence of years. For example, if a 40-year sequence of years existed all with 0.5 K anomalies eleven 30-year sequences would result. To prevent this, once a given sequence was identified the search routine skipped the next 30 or 100 years from the *end* of the identified sequence.

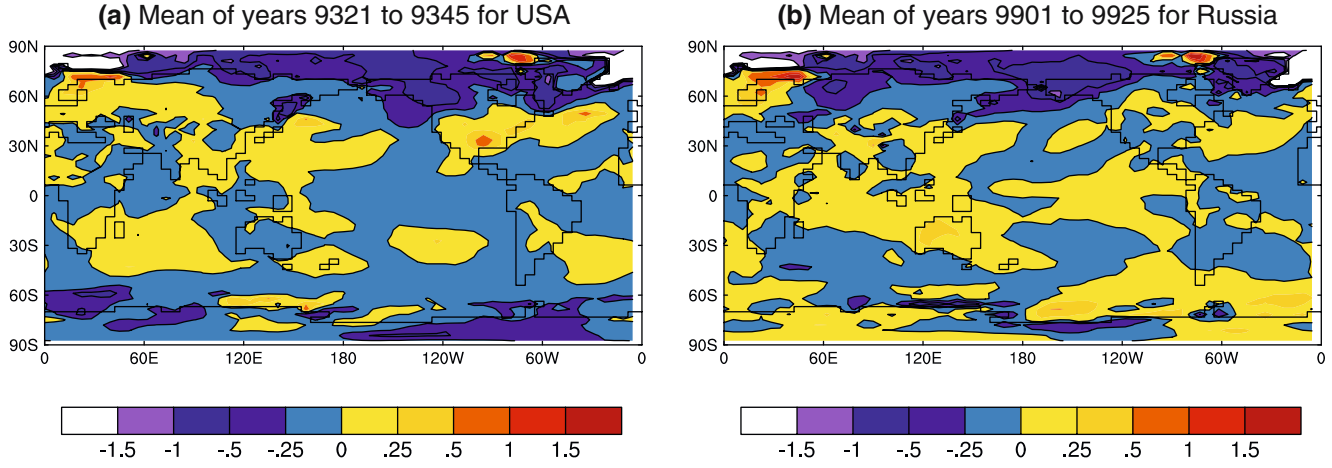

Fig. 5 Global distributions of annual mean surface temperature anomalies averaged over separate 25-year periods associated with the time series shown in Fig. 4. Panel **a** is for the positive anomalies in Fig. 4 **a**, and highlights a warm interval over the USA. Panel **b** is for the negative anomalies in Fig. 4 **b**, and highlights a cold interval over western Russia and much of Asia. The *colour bars* are in K

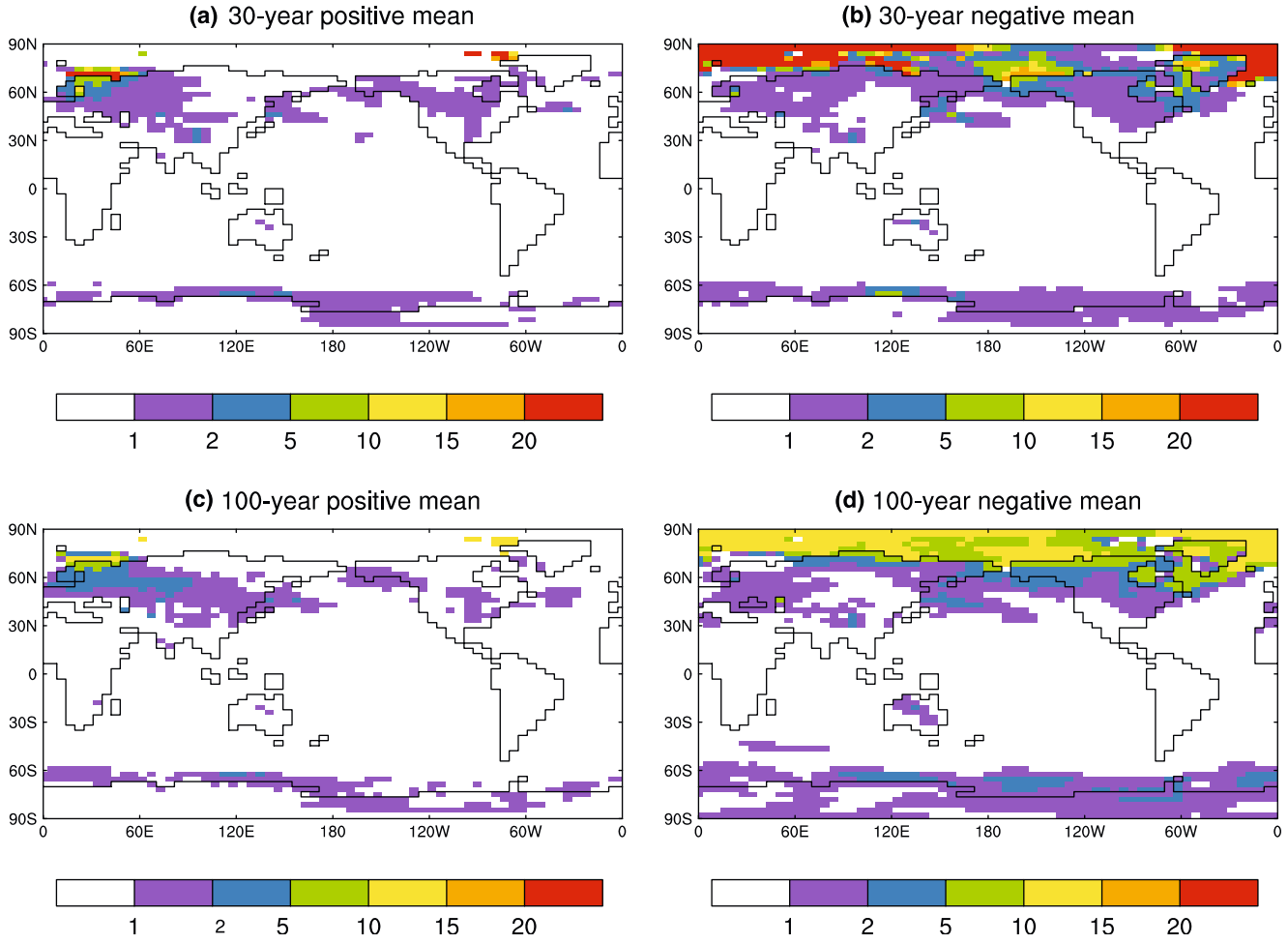

Fig. 6 The frequency of occurrence *per millennium* for annual mean temperature anomalies with defined characteristics. The 30-year duration periods had mean anomalies greater than |0.5 K| while the 100-year duration periods had mean anomalies greater than |0.2 K|. Results are given for individual gridboxes for the period 9,001–10,000 years of the simulation. The *colour bars* give the counts *per millennium*

While the results in Fig. 6 are all for the millennium 9,001–10,000 years of the simulation, the patterns obtained were very similar for other millennia, essentially only details varied. It needs to be appreciated that where single occurrences are associated with the individual gridboxes, this does not imply simultaneity of occurrence of the specified event. Only adjacent gridboxes tended to record simultaneous events, while the events for other gridboxes could be widely separated in time.

The remarkable outcome in Fig. 6 is the restriction of events to primarily northern hemispheric land, and sea–ice in both hemispheres. For all four cases in Fig. 6, over the majority of the globe, especially the oceans, no sequences could be found that met the specified criteria. Tightening the search criteria significantly changed the outcomes. For example, very few gridboxes were identified for 30-year duration trends with a mean anomaly of ± 1 K, compared with the 30-year, ± 0.5 K criterion used in Fig. 6. The criteria used in Fig. 6 were considered to constitute reasonable ranges given the variability of observed time series. Excluding Antarctica, sequences in the southern hemisphere were essentially only found over Australia. This again emphasises the hemispheric asymmetry of naturally occurring climatic variability, and, presumably the different climatic mechanisms operating in the two hemispheres.

This may reflect model deficiencies, as observations indicate temperature anomalies in the southern hemisphere, which, if they had occurred in the model, would have been captured in the analysis used to generate Fig. 6. Thus, Cook et al. (2000) present a 3,600-year dendroclimatological time series of temperature for Tasmania that indicates a MWP-type warming, but no LIA-type cooling. While Fig. 6 reveals multi-decadal duration warming and cooling episodes over Australia, the failure to obtain a corresponding signal over Tasmania is probably because the coarse horizontal resolution of the model cannot reproduce the required regional climatology. Cook et al. (2000) also show a 1,400-year time series of warm season sea-surface temperature anomalies (primarily in the range ± 0.2 K) for the southern Indian Ocean from a simulation with the

UK HADCM2 coupled model. They state that the model's decadal and century timescales were remarkably similar to their Tasmanian observations, while also noting that this was an unforced model simulation.

Also, presumably because of the highly smoothed orography in the present R21 model, Fig. 6 fails to reproduce the observed cooling coincident with the LIA reported by Villalba et al. (2002) for South America.

No signal is shown is Fig. 6 for the tropical Pacific Ocean even though temperature time series derived by Cobb et al. (2003) and Lough and Barnes (1997) from corals indicate some support for the LIA. However, Cobb et al. whose results cover part of the MWP do not show any warming for this period. Interestingly, they also state that over the last 1,000 years the majority of ENSO variability may be attributable to internal ENSO dynamics.

Only one sequence was found for either the 30- or 100-year duration events for most locations in a given millennium. This rarity reflects the difficulty that the unforced climatic system has in sustaining long-term anomalies. The biggest exception to this outcome was over the Arctic cap, where sequences of negative anomalies were quite prevalent. Apart from Europe and Alaska there were only a few isolated gridboxes where more than one event was identified. This outcome is consistent with the results in Fig. 3 and 5 for Russia. The net result from Fig. 6 is that only one event of the specified outcome is likely to occur *per millennium* at most locations, with large regions of the globe failing to record even a single event.

Time series of surface temperature anomalies for all 10,000 years of the simulation were made for gridboxes in Africa, Australia, South America and the oceans to determine why these regions, with the exception of Australia, recorded zero signals in Fig. 6. Over Africa, South America and the oceans the principal reason was that most temperature anomalies were too small, below 0.5 K, hence the search criteria could not be met. Over Australia, where small response regions can be seen in Fig. 6, anomalies above 1.0 K were quite frequent, but the variability was dominated by fluctuating interannual events, presumably attributable to ENSO events. Thus few *sustained* runs of anomalies of a given sign prevailed.

In Fig. 7 examples are given of simulated time series of surface temperature anomalies for a gridbox in the USA, and a gridbox in Russia which met the criteria of having a 100 years sequence of *mean* temperatures above 0.2 K and below −0.2 K, respectively. Global temperature anomalies averaged over two (different) 100-year periods are illustrated in the lower part of Fig. 7. As expected (Hunt 2004), both of the time series have both positive and negative anomalies for the identified 100-year periods. The cold period over Russia is somewhat more clearly defined than the warm period over the USA in Fig. 7.

In accordance with the search criterion of 100-year mean temperature anomalies of ± 0.2 K, the temperature anomalies shown in the lower panels of Fig. 7 are modest. For the warm USA case, Fig. 7c, an extended swathe of positive temperature anomalies occurs from the west coast of the USA eastwards across the Atlantic, Europe, Asia and into the northwest Pacific, implying substantial synchronicity in this period. However, synchronicity did not always exist between the responses in Russia and the USA in other 100-year periods. A particularly marked warming anomaly occurred over Scandinavia and northwest Russia in this example. No outstanding anomalies were located in the southern hemisphere except over the sea–ice.

In the cold Russian case, Fig. 7d, a somewhat larger negative temperature anomaly, compared to the warm USA case, can be seen over a large part of that country. While a synchronous negative temperature anomaly was located over Canada, positive anomalies occurred over part of Siberia and the Alaskan region, hence there was less synchronicity overall than in Fig. 7c. Again, little response can be seen in the southern hemisphere.

An examination of time-averaged spatial plots for 30-year periods with mean temperature anomalies greater than ± 0.5 K (not shown), revealed similar regional outcomes to those in Fig. 7, but, of course, with larger temperature anomalies.

In summary, sustained periods of above or below average temperatures with large spatial scales can be produced in unforced climatic simulations. Such periods have both positive and negative temperature anomalies, but with one anomaly type dominating, and provide climatic conditions that could give rise to such concepts as the MWP or the LIA.

4 Regional climatic issues

An attempt was made to identify cold episodes over Europe that could be related to recorded advances of glaciers in the LIA (Grove 1998). Given that the occurrence of these glaciers is associated with mountainous valleys, the coarse horizontal resolution of the model precluded any useful outcome. Nevertheless, it would be valuable to use the output from a global model to drive an appropriate fine-scale regional model to investigate this aspect in more detail.

An examination was also made of precipitation/surface temperature relationships at individual model gridboxes. Grove (1998) reported that in *some decades* during the LIA in Europe cool, wet summers and cold, dry winters prevailed. For a model gridbox in Russia (60°N, 60°E) this situation was investigated in some detail. Over all 10,000 years of the simulation the correlation coefficient between precipitation and surface temperature for *annual* conditions was 0.14, while for July it was only 0.015. Comparison of these time variables for short time sections, typically revealed multi-decadal intervals where cool/dry, warm/dry and cool/wet sequences could be identified. No compelling evidence of specific MWP or LIA relationships was

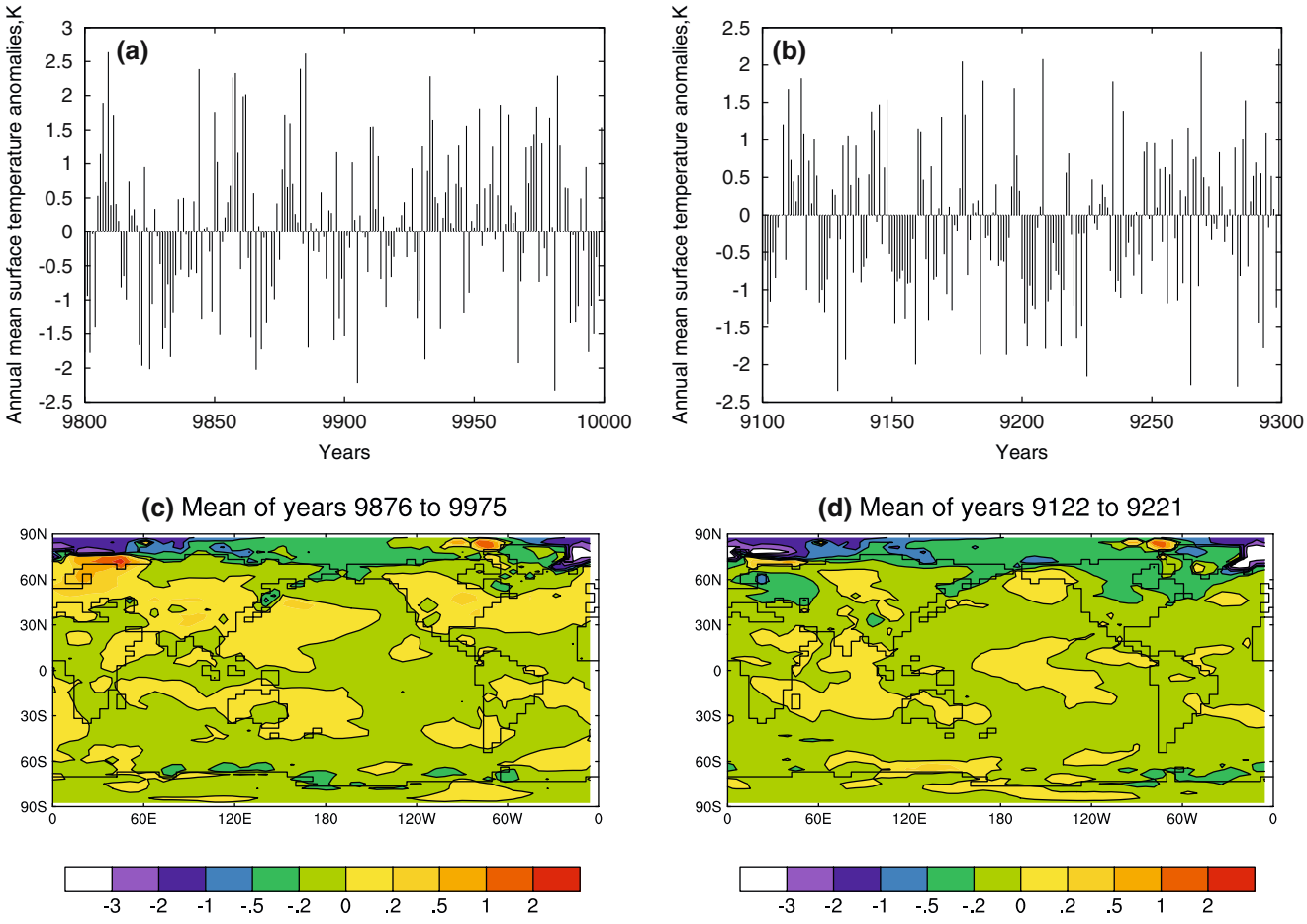

Fig. 7 The *upper panels* show time series of annual mean surface temperature anomalies. Panel **a** has results for a USA gridbox (50°N, 90°W) where a 100-year period occurred with a mean anomaly greater than 0.2°K. Panel **b** has corresponding results for a Russian gridbox (50°N, 30°E) with a mean anomaly below −0.2°K. The *lower panels* illustrate global distributions of annual mean surface temperature anomalies averaged over 100-year periods, where the mean anomalies were above 0.2°K or below −0.2°K, respectively for the gridboxes identified in the *upper panels*. The years over which the averages were taken are identified on the *lower panels*. Note the different periods for the two locations. The *colour bars* are in K

apparent, in agreement with the low-valued correlation coefficients.

Again, Cook et al. (2004), based on tree-ring records, have identified severe drought conditions over western North America with the MWP, defined by them as 900–1300 AD. They did not, however, present corresponding temperature values. An analysis for this region using the model output was marginally supportive of a relationship between reduced rainfall and above average temperatures. For example, using annual mean values the correlation coefficient between surface temperature and precipitation for this region was only −0.199 based on all 10,000 years of the simulation. Only one or two century long periods were found with reasonably persistent drought and warm conditions, in agreement with the null result for western North America in Fig. 6.

The analysis of Cook et al. (2004) was based on 60-year band pass filtering. When the model output was similarly filtered the correlation coefficient between surface temperature and precipitation increased to −0.210, as compared with a reduced value of −0.108 for 60-year running means. This processing produced some century or longer 'drought episodes' on a few occasions but this aridity was not consistently related to warmer surface temperatures. Cook et al. (2004) also present a number of millennial length smoothed time series representative of aridity in western North America, but these revealed some temporal inconsistencies, again indicating lack of spatial homogeneity in the occurrence of aridity for the period 900–1300 AD.

A further aspect of regional climatic variability examined was that of sea–ice variability. Following Koslowski and Glaser (1999), who produced a rather coarse index of winter ice extent for the Baltic Sea, a time series of sea–ice thickness is presented in Fig. 8 for the Baltic Sea from the simulation. This shows very large interannual fluctuations upon which are superimposed decadal and longer-term variations. Of particular note in Fig. 8 are individual decades of high sea–ice thickness (implying extended areal extent), together with multi-decadal periods of very reduced thickness, all generated by natural variability. Rather similar fluctuations are

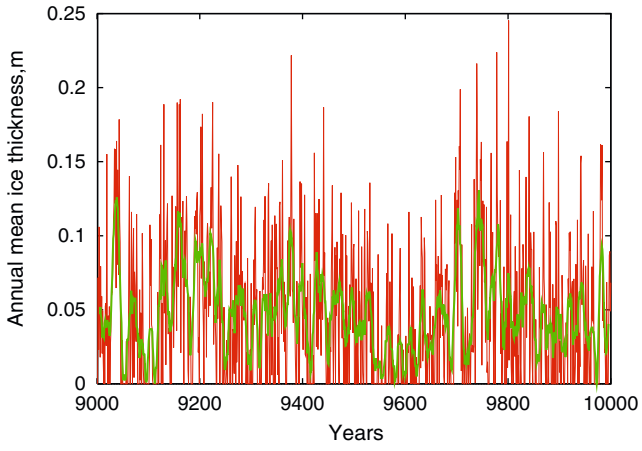

Fig. 8 Time series of annual mean sea–ice thickness for a model gridbox in the Baltic Sea (60°N, 25°E) is illustrated for the period 9,001–10,000 years of the simulation by the *red lines*. The *green line* shows a 10-point running mean

apparent in the smoothed time series of Koslowski and Glaser (1999), suggesting that the model has captured this feature surprisingly well.

In order to test for more persistent sea–ice anomalies results were averaged for the periods 9,876–9,975 and 9,122–9,221, the same timeframes as used in Fig. 7. These timeframes were associated with generally warm and cold conditions respectively over North America and northwest Russia.

Figure 9 compares the global sea–ice anomalies averaged over these centennial periods and for January, February and March. For the warm episode, years 9,876–9,975, sustained negative anomalies in sea–ice occurred in the Baltic, along most of the Arctic coastline of Russia and northwest Greenland, while positive anomalies elsewhere in the Arctic were very low. In contrast, for the cold episode, years 9,122–9,221 in Fig. 9 there were positive anomalies across the whole of the Arctic Ocean, except for a very small region north of Norway. Elsewhere over the globe rather small-scale sea–ice changes occurred around Antarctica, off the coast of Siberia and in the Labrador–Greenland region. Zorita et al. (2004) obtained very large increases in ice extent over the North Atlantic, south of Greenland, in a simulation of the Late Maunder Minimum.

The important outcome as far as the simulation is concerned is that long duration sea–ice anomaly changes can be identified that are attributable to natural variability.

Observational studies of the secular variability of sea–ice in the European region suggest a range of outcomes. For example, around Iceland sea–ice variations appear to be dominated by annual to possibly decadal timescales (Ogilvie 1984). The model was unable to generate sea–ice in the vicinity of Iceland as its resolution is too coarse to reproduce the necessary oceanic current systems.

5 Mechanistic analysis

While the extended periods of positive and negative temperature anomalies identified in Fig. 4 and 7 are attributable to simulated naturally occurring climatic variability it is important to identify whether such variability can be related to specific climatic phenomena. Given the spatial patterns of temperature anomalies in the northern hemisphere a relationship to the North Altantic Oscillation (NAO) might be expected (Hurrell 1995).

In Fig. 10 the simulated NAO index for winter conditions (mean of December, January, February and March) has been correlated with the corresponding global winter surface temperature for three different periods. The NAO index used here was defined as the surface pressure at a gridbox near the Azores (37.8°N,

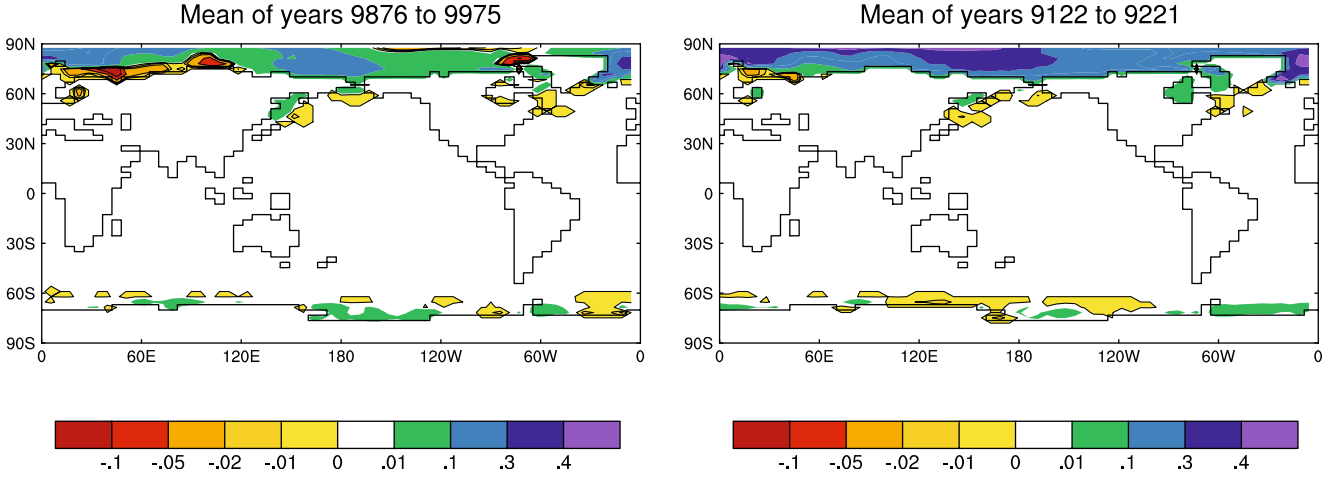

Fig. 9 The January, February and March mean sea–ice anomalies averaged over the years 9,876–9,975 and 9,122–9,221 are shown in the *left* and *right hand panels*, respectively. These periods correspond to the warm and cold episodes shown in the lower part of Fig. 7. The *colour bars* are in metres

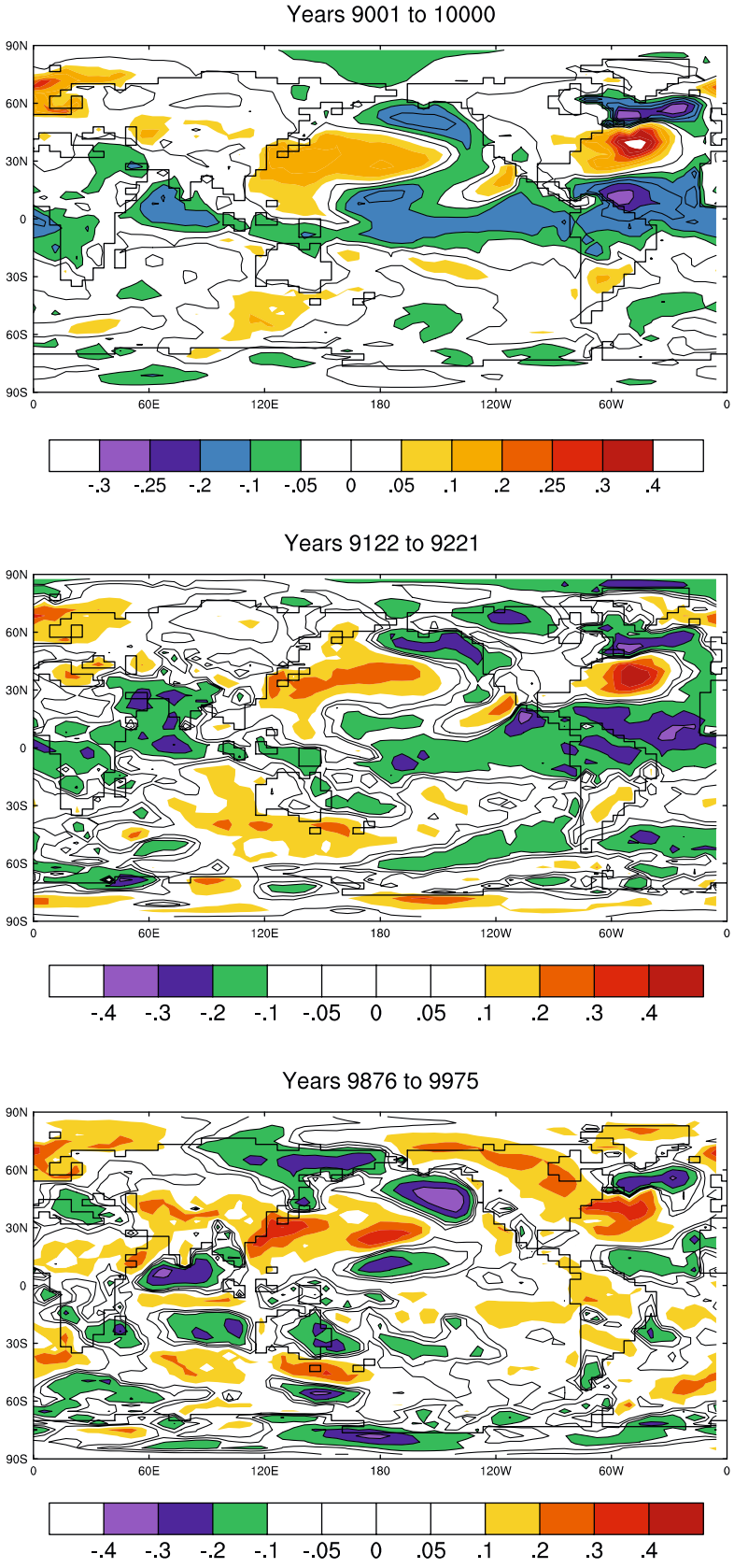

Fig. 10 Correlation of the NAO index with the global surface temperature for three periods of the 10,000-year simulation. The *upper panel* is for the millennium 9,001–10,000, the *middle panel* for a cold period over Russia and the *lower panel* for a warm period over the USA and Russia (see Fig. 7). Results are for winter conditions (December, January, February and March). The *colour bars* give the value of the correlation coefficient. Regions left white have values below the 90% significance level

334.3°E) minus the surface pressure at a gridbox near Iceland (65.1°N, 337.3°E). The upper panel in Fig. 10 illustrates the correlation for the 1,000-year period 9,001–10,000 years, of the simulation. The basic pattern is quite similar to the observed correlation (Marshall et al. 2001) for 1864–1994. The principal difference is

that the simulated correlation values were smaller than the observed values. However, the simulated pattern was not particularly stable, and substantial differences were apparent in the corresponding correlations for the millennium 8,001–9,000 years (not shown) for the North Pacific, North America, western Eurasia and Australia.

The variability of the correlation pattern is highlighted in the second and third panels in Fig. 10, where results are shown for two different century long periods associated with warm and cold episodes in northwest Europe, see Fig. 7. While the two upper panels in Fig. 10 are fairly similar, the lower panel, for the warmer century, was noticeably different over North America, the tropical Atlantic and Pacific Oceans, Australia and the Mediterranean. It would be interesting to know whether such variability exists in longer-term observations than are currently available.

The role of the NAO was examined by comparing time series of the NAO with time series of surface temperature for a point in eastern Russia, for the sustained warming and cooling episodes over Russia in Fig. 7c, d. No compelling agreement was found. This may be attributable to the instability of the NAO index, as Stephenson et al. (2000), amongst others, have concluded that the observed winter NAO index has the characteristics of white noise. Fitting an auto-regressive function to individual millennial length time series of the simulated NAO index produced an AR series of order zero, indicating white noise. Collins et al. (2001) also found limited agreement between their simulated NAO and observations, as did Zorita et al. (2004).

Given the white noise nature of the NAO, the question arises whether the NAO has a forcing role in climatic perturbations (Hurrell 1995; Thompson and Wallace 1998), or whether it is just part of the overall mutual reaction of the climatic system. Certainty, it seems difficult to ascribe a major causative role to the NAO as regards the climatic variations associated with the MWP or LIA, but this could be indicative of model deficiencies.

Given the occurrence of extended temperature anomalies over North America, Fig. 4 and 7, a search for a causative mechanism was also conducted for this region. Two important phenomena in the Pacific Ocean, the El Niño/Southern Oscillation (ENSO), and the Pacific Decadal Oscillation (PDO), were examined.

Figure 11 illustrates the correlation, over years 9,001–10,000 of the simulation, between the NINO3.4 region (5°S–5°N, 170–120°W) sea surface temperature and surface temperature over the whole globe. The correlation pattern for the Pacific Ocean is typically that associated with ENSO events. Interestingly, there is a local (negative) maximum correlation over much of North America, suggesting that temperature variability over this region is forced by ENSO activity. A similar feature is obtained in the observational regression pattern produced by Collins et al. (2001), but not in their simulation. The correlation pattern in Fig. 11 substantially agrees with the above observational pattern. Any ENSO influence is much weaker over Europe in Fig. 11, indicating that it is not responsible for the simulated, long-term temperature anomalies in this region shown in Fig. 7. A more detailed analysis of the ENSO climatology of the present model is given in Hunt and Elliott (2003).

The possible forcing of the sustained warming episode over North America (years 9,876–9,975 shown in Fig. 7) by the NINO3.4 sea surface temperature variations was investigated. Figure 12a compares the NINO3.4 time series with a surface temperature time series for a gridbox (45°N, 80°W) near the centre of the negative correlation over North America shown in Fig. 11. While over the 10,000 years of the simulation the correlation between these time series was −0.289, the implied relationship shown in Fig. 12a is not particularly compelling given the amplitude of the NINO3.4 anomalies. The relationship between this gridbox surface temperature and the PDO shown in Fig. 12b (10,000-year correlation of −0.233) is even less convincing. This outcome, however, could be attributable to the modest amplitude of ENSO surface temperature anomalies in the simulation, typically one-half to two-thirds of observed values. Interestingly, both ENSO and the PDO were found to be associated with a megadrought over the USA simulated in the present model (Hunt 2005), in agreement with the observations of Cole et al. (2002). In both cases stochastic processes were deemed to be important for the megadrought.

Examination of other century long periods, where the US temperature variability was dominated by *multi-annual* fluctuations, revealed somewhat clearer anti-correlations between the two time series. The NINO3.4 temperature anomalies were larger for these situations. Thus the *extended* periods of positive and negative temperature anomalies over North America arise when the NINO3.4 'forcing' is weaker. This implies that local influences predominate at such times.

As expected, the surface temperature changes were negatively correlated with the total cloud amount, typically at the − 0.3 to − 0.4 levels. Assuming that the cloud changes are the precursors to the surface temperature changes, examination of the global plots, composites and time means, and time series of surface pressure, atmospheric temperatures and circulation did not identify any specific features that could explain why warming or cooling episodes, such as shown in Fig. 7, were generated.

Given that the wide range of climatic fluctuations in the model simulation presented here and elsewhere (Hunt and Elliott 2003, 2005) are a consequence of naturally occurring climatic variability, then the simplest and most plausible explanation for the MWP and LIA related results documented here is that they are attributable to stochastic influences. While there are coupled processes, such as ENSO, operative within the simulation, the decade-to-decade, and century-to-century variations of such processes are also attributable to stochastic influences (see Blanke et al. 1997; Eckert and

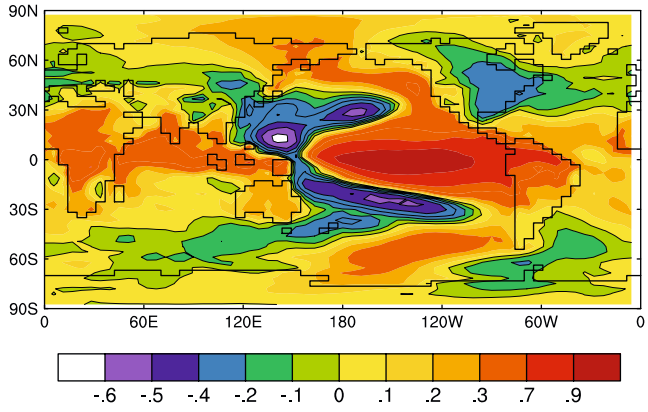

Fig. 11 Correlation of the NINO3.4 sea surface temperature with the global surface temperature distribution for years 9,001–10,000 of the simulation. Results are for annual mean conditions. The *colour bar* gives the value of the correlation coefficient

Latif 1997 and Delworth and Greatbatch 2000). The extended duration warm and cold events displayed in Fig. 7 are a consequence of the preponderance of anomalies of one sign, rather than a monotonic sequence of anomalies, thus the time series are still characteristic of stochastic influences. The infrequency of these events, as identified in Fig. 6, implies that they are, however, near the extreme limit of stochastic forcing. This indicates that external forcing appears to be necessary to account for the sustained temperature anomalies associated with the MWP and LIA.

6 Concluding remarks

It has been shown, in agreement with some earlier simulations, that the present coupled model can reproduce many of the climatic perturbations associated with the concepts of the MWP and the LIA. Whether these phenomena actually occurred as distinct climatic events is still a matter of debate (Jones and Mann 2004). Nevertheless, observational studies clearly document climatic anomalies over the last millennium that were of considerable amplitude and spatial extent, even if they were not contemporaneous. The present simulation has been used to document such anomalies and to provide both a global and lengthy temporal perspective.

Thus, for specific climatic events in both Europe and the USA it was shown that the model was capable of reproducing the observed characteristics, (Fig. 2). Furthermore, examples were given (Fig. 4), of 25-year duration positive and negative surface temperature anomalies that could, if observed, have contributed to the perceptions of the MWP and LIA. Extensive spatial patterns were associated with the time average of these anomalies (Fig. 5), but synchronicity was not obtained on a global or even a hemispheric basis.

The simulation was not capable of producing some of the observed centennial or longer time series of monotonic surface temperature anomalies. However, the simulation did generate 100-year time series of such anomalies with rather modest time averaged values, and distinctive spatial patterns (Fig. 7). Nevertheless, the larger amplitude of the observed temperature anomalies and their longer durations suggest that external forcing is required to sustain them.

A global search of the simulation for either 30- or 100-year time averaged surface temperature anomalies of specified magnitudes produced the surprising outcome that such events were not generated over the majority of the globe, expressly the oceans and most of the southern hemispheric land areas, Fig. 6. These events were restricted to the polar regions and the

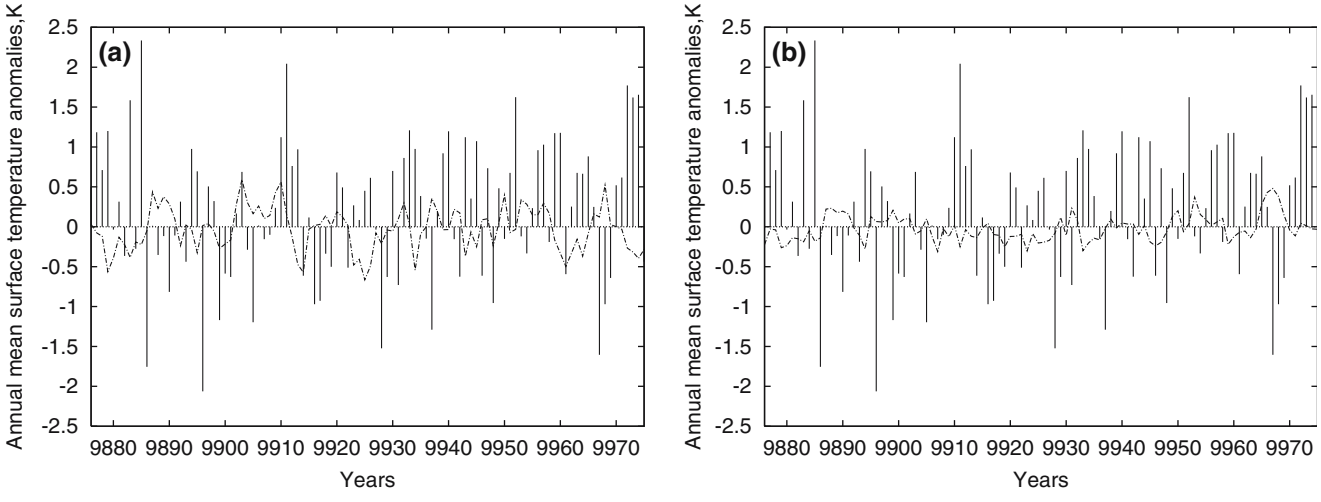

Fig. 12 Time series of surface temperature anomalies for a US gridbox (45°N, 80°W), corresponding to the warm episode over the USA for years 9,876–9,975 (see Fig. 7 a), is illustrated by the *full*, *vertical lines* in the two panels. In panel **a** the *dashed lines* are the sea surface temperature anomalies for the NINO3.4 region, while in panel **b** the *dashed lines* correspond to the PDO index

northern parts of Europe, Asia and North America. In general, only one event per millennium was identified. The spatial outcome resulted either from the surface temperature anomalies being too small (over the oceans) or dominated by multi-annual events (southern hemispheric land).

Substantial, sustained sea–ice fluctuations, that broadly agreed with observations, were also obtained in the simulation.

In an examination of possible forcing mechanisms for the simulation of long-term climatic fluctuations, no compelling evidence was obtained to relate these fluctuations to the North Atlantic Oscillation, ENSO or the PDO. Hence, it is concluded that the various climatic fluctuations documented in this paper are attributable to stochastic forcings intrinsic to the nonlinear mechanisms governing climatic evolution. Thus, they are all examples of naturally occurring climatic variability. Observationally, external forcing would be expected, however, to project unto such large-scale modes.

In the actual climatic system, large volcanic eruptions undoubtedly contributed to past climatic coolings. As such, they would account for some of the observed multi-annual extreme negative temperature anomalies, a feature the model did not simulate. A colder overall climate would have been simulated if greenhouse gas concentrations prior to the industrial revolution had been used (Rind et al. 2004), which might have improved agreement with observations.

The question regarding the role (if any) for solar perturbations inducing climatic fluctuations is a matter of concern, especially following the observational analysis of Turney et al. (2005). If it eventuates, and this remains to be confirmed, that solar perturbations have little or no influence, then a substantial reassessment of current explanations of climatic fluctuations over the past millennium will be necessary. It may be possible to account for the vagaries of the LIA by the combined roles of greenhouse gas variations, large volcanic eruptions and internal climatic variability, but not the MWP. Certainly, more numerous and improved reconstructions of MWP temperatures would help to establish what temperature anomalies have to be explained. Future improvements in climatic models may also provide better simulations of past climate. This might arise, for example, as a consequence of greater sensitivity to external forcing generating larger climatic anomalies than presently obtained.

A more intriguing possibility is that by developing models that are not as tightly constrained to present climatic conditions as current models, a wider range of internal climatic variability could result.

References

AchutaRao K, Sperber KR (2000) El Nino Southern Oscillation in coupled models. PCDMI Rep 61, PCDMI, Lawrence Livermore National Laboratory, Livermore

Beer J, Mende W, Stellmacher R (2000) The role of the sun in climate forcing. Quat Sci Rev 19:403–415

Bell JL, Sloan LC, Revenaugh J, Duffy PB (2003) Evaluation of northern hemisphere natural climate variability in multiple temperature reconstructions and global climate model simulations. Glob Planet Change 37:19–32

Bertrand C, Loutre MF, Crucifix M, Berger A (2002) Climate of the last millennium: a sensitivity study. Tellus 54A:221–244

Biondi F, Perkins DL, Cayan DR, Hughes MK (1999) July temperatures during the second millennium reconstructed from Idaho tree rings. Geophys Res Lett 26:1445–1448

Blanke B, Neelin JD, Gutzler D (1997) Estimating the effect of stochastic wind stress forcing on ENSO irregularity. J Clim 10:1473–1486

Bradley RS, Hughes MK, Diaz HF (2003) Climate in medieval time. Science 302:404–405

Brazdil R, Pfister C, Wanner H, von Storch H, Luterbacher J (2005) Historical climatology in Europe–the state of the art. Clim Change 70:363–430

Briffa KR, Osborn TJ, Schweingruber FH (2004) Large-scale temperature inferences from tree rings: a review. Global Planet Change 40:11–26

Broecker WS (2001) Was the medieval warm period global? Science 291:1497–1499

Cobb KM, Charles CD, Cheng H, Edwards RL (2003) El Nino/Southern Oscillation and tropical Pacific climate during the last millennium. Nature 424:271–276

Cole JE, Overpeck JT, Cook ER (2002) Multiyear La Niña events and persistent drought in the contiguous United States. Geophs Res Lett. 29, No.13 10.1029/2001GL013561

Collins M, Tett SFB, Cooper C (2001) The internal climate variability of HadCM3, a version of the Hadley Centre coupled model without flux adjustments. Clim Dyn 17:61–81

Collins M, Osborn TJ, Tett SFB, Briffa KR, Schweingruber FH (2002) A comparison of the variability of a climate model with palaeotemperature estimates from a network of tree-ring densities. J Clim 15:1497–1515

Cook ER, Buckley BM, D'Arrigo RD, Peterson MJ (2000) Warm-season temperatures since 1600 BC reconstructed from Tasmanian tree rings and their relationship to large-scale surface temperature anomalies. Clim Dyn 16:79–91

Cook ER, Woodhouse CA, Eakin CM, Meko DM, Stahle DW (2004) Long-term aridity changes in the western United States. Science 305:1015–1018

Covey C, AchutaRao KM, Lambert SJ, Taylor KE (2000) Intercomparison of present and future climates simulated by coupled ocean–atmosphere GCMs. PCDMI Rep 66, PCDMI, Lawrence Livermore National Laboratory, Livermore

Cronin TM, Twyer GS, Kamiya T, Schwede S, Willard DA (2003) Medieval warm period, little ice age and 20th century temperature variability from Chesapeake Bay. Global Planet Change 36:17–29

Crowley TJ, Kim K-Y (1999) Modelling the temperature response to forced climate change over the last six centuries. Geophys Res Lett 26:1901–1904

Damon PE, Laut P (2004) Pattern of strange errors plagues solar activity and terrestrial climate data. EOS (Trans Amer Geophys Union) 85:370 and 374

D'Arrigo R, Jacoby G, Frank D, Pederson N, Cook E, Buckley B, Nachin B, Mijiddorj R, Dugarjav C (2001) 1738 years of Mongolian temperature variability inferred from a tree-ring width chronology of Siberian pine. Geophy Res Lett 28:543–546

Davies HL, Hunt BG (1994) The problem of detecting climatic change in the presence of climatic variability. J Met Soc Japan 72:765–771

Delworth TL, Greatbatch RJ (2000) Multidecadal thermohaline circulation variability driven by atmospheric surface flux forcing. J Clim 13:1481–1494

Diaz HF, Pulwarty RS (1994) An analysis of the time scales of variability in centuries-long ENSO-sensitive records in the last 1000 years. Clim Change 26:317–342

Eckert C, Latif M (1997) Predictability of a stochastically forced hybrid coupled model of El Niño. J Clim 10:1488–1504
Esper J, Wilson RJS, Frank DC, Moberg A, Wanner H, Luterbacher J (2005) Climate: past ranges and future changes. Quat Sci Rev 24:2164–2166
Felis F, Patzold J. (2004) Corals as climate archive. In: Fisher H, Kumke T, Lohmann G, Floser G, Miller H, von Storch H, Negendank JFW (eds) The climate in historical times. Springer, Berlin Heidelberg New York, pp 91–108
Foukal P, North G, Wigley T (2004) A stellar view on solar variations and climate. Science 306:68–69
Goosse H, Renssen H, Timmermann A, Bradley RS (2005) Internal and forced climate variability during the last millennium: a model-data comparison using ensemble simulations. Quat Sci Rev 24:1345–1360
Gordon HB, O'Farrell SP (1997) Transient climate change in the CSIRO coupled model with dynamic sea ice. Mon Weather Rev 125:875–907
Graumlich LJ (1993) A 1000-year record of temperature and precipitation in the Sierra Nevada. Quat Res 39:249–255
Grove JM (1998) The Little Ice Age. Methuen, London
Hirst AC, O'Farrell SP, Gordon HB (2000) Comparison of a coupled ocean–atmosphere model with and without oceanic eddy induced advection. Part I ocean spinup and control integrations. J Clim 139–163
Hodell DA, Brenner M, Curtis JH, Guilderson T (2001) Solar forcing of drought frequency in the Maya Lowlands. Science 292:1367–1370
Hughes MK, Diaz HF (1994) Was there a 'Medieval Warm Period', and if so, where and when? Clim Change 26:109–142
Hunt BG (1998) Natural climatic variability as an explanation of historical climatic fluctuations. Clim Change 38:133–157
Hunt BG (2001) A description of persistent climatic anomalies in a 1000-year climatic model simulation. Clim Dyn 17:717–733
Hunt BG (2004) The stationarity of global mean climate. Int J Climatol 24:795–806
Hunt BG (2005) Climatological extremes of simulated annual mean rainfall. J Clim (in press)
Hunt BG, Elliott TI (2002) Mexican megadrought. Clim Dyn 20:1–12
Hunt BG, Elliott TI (2003) Secular variability in ENSO events in a 1000-year climatic simulation. Clim Dyn 20:689–703
Hunt BG, Elliott TI (2005) A simulation of the climatic conditions associated with the collapse of the Maya civilization. Clim Change 69:393–407
Hurrell JW (1995) Decadal trends in the North Atlantic Oscillation: regional temperatures and precipitation. Science 269:676–679
IPCC (2001) Climate change 2001: the scientific basis. Houghton JT, Ding Y, Griggs DJ, Noguer M, van der Linden PJ, Dai X, Maskell K, Johnson CA (eds) Cambridge University Press, Cambridge pp 99–181
Jones PD, Briffa KR, Barnett TP, Tett SFB (1998) High-resolution paleoclimatic records for the last millennium: interpretation, integration and comparison with general circulation model control-run temperatures. Holocene 8:455–471
Jones PD, Mann ME (2004) Climate over past millennia. Rev Geophys 42(2):1–42
Keigwin LD (1996) The little ice age and medieval warm period in the Sargasso Sea. Science 274:1505–1508
Koslowski G, Glaser R (1999) Variations in reconstructed ice winter severity in the western Baltic from 1501 to 1995, and their implications for the North Atlantic Oscillation. Clim Change 41:175–191
Lean JL, Wang Y-M, Sheeley NR (2002) The effect of increasing solar activity on the Sun's total and open magnetic flux during multiple cycles: implications for solar forcing of climate. Geophys Res Lett 29(24): 2224, DOI 10.1029/2002GL015880
Lough JM, Barnes DJ (1997) Several centuries of variation in skeletal extension, density and clarification in massive Porites colonies from the Great Barrier Reef: a proxy for seawater temperature and a background of variability against which to identify unnatural change. J Exp Mar Biol and Ecol 211:29–67
Luterbacher J, Dietrich D, Xoplaki E, Grosjean M, Wanner H (2004) European seasonal and annual temperature variability, trends, and extremes since 1500. Science 303:1499–1503
Mann ME, Bradley RS, Hughes KS (1998) Global-scale temperature patterns and climate forcing over the past six centuries. Nature 392:779–787
Mann ME, Bradley RS, Hughes MK (1999) Northern hemisphere temperatures during the past millennium: inferences, uncertainties and limitations. Geophys Res Lett 26:759–762
Marshall J, Kushnir Y, Battisti D, Chang P, Czaja A, Dickson R, Hurrell J, McCartney M, Saravanan R, Visbeck M (2001) North Atlantic climate variability: phenomena, impacts and mechanisms. Int J Climatol 21:1863–1898
Ogilvie AEJ (1984) The past climate and sea–ice record from Iceland. Part I. Data to AD 1780. Clim Change 6:131–152
Petersen KL (1994) A warm and wet little climatic optimum and cold and dry little ice age in the southern Rocky Mountains, USA. Clim Change 26:243–269
Rind D, Overpeck J (1993) Hypothesized causes of decade-to-century-scale climate variability: climate model results. Quaternary Sci Rev 12:357–374
Rind D, Shindell D, Perlwitz J, Lerner J, Lonegan P, Lean J, McLinden C (2004) The relative importance of solar and anthropogenic forcing of climate change between the Maunder Minimum and present. J Clim 17:906–928
Ruddiman WF (2005) Plows plagues and petroleum. Princeton University Press, Princeton
Sausen R, Barthel K, Hasselmann K (1988) Coupled ocean–atmosphere models with flux correction. Clim Dyn 2:145–163
Serre-Bachet F (1994) Middle ages temperature reconstructions in Europe: a focus on northeastern Italy. Clim Change 26:213–224
Shindell DT, Schmidt GA, Miller R, Mann ME (2003) Volcanic and solar forcing of climate change during the preindustrial era. J Clim 16:4094–4107
Shindell DT, Schmidt GA, Mann ME, Faluvegi G (2004) Dynamic winter climate response to large tropical volcanic eruptions since 1600. J Geophys Res 109: D05104. DOI 10.1029/2003JD004151
Stephenson DB, Pavan V, Bojarus R (2000) Is the North Atlantic Oscillation a random walk? Inter J Climatol 20:1–18
von Storch H, Zorita E, Jones JM, Dimitriev Y, Gonzalez-Rouco F, Tett SFB (2004) Reconstructing past climate from noisy date. Science 306:679–682
Thompson DWJ, Wallace JM (1998) Observed linkages between Eurasian surface air temperatures, the North Atlantic Oscillation, Arctic sea-level pressure and the stratospheric polar vortex. Geophys Res Lett 25:1297–1303
Turney C, Baillie M, Clemens S, Brown D, Palmer J, Pilcher J, Reimer P, Leuschner HH (2005) Testing solar forcing of pervasive Holocene climate cycles. J Quat Sci 20:511–518
Villalba R (1994) Tree-ring and glacial evidence for the medieval warm epoch and the little ice age in southern South America. Clim Change 26:183–197
Villalba R, Lara A, Bonisegna JA, Areana JC, Roig F, Schmelter A, Delgado S, Wolodarscky A, Riplata A (2002) Large-scale temperature changes across the southern Andes 20th-century variations in the context of the past 400 years. Clim Change 59:177–232
Wagner S, Zorita E (2005) The influence of volcanic, solar and CO_2 forcing on the temperature in the Dalton Minimum (1790–1830) a model study. Clim Dyn 25:205–218
Waple A, Mann ME, Bradley RS (2002) Long-term patterns of solar irradiance forcing in model experiments and proxy-based surface temperature reconstructions. Clim Dyn 18:563–578

Zorita E, von Storch H, Gonzalez-Rouco FJ, Cubasch U, Luterbacher J, Legutke S, Fischer-Bruns I, Schlese U (2004) Climate evolution in the last five centuries simulated by an atmosphere–ocean model: global temperatures, the North Atlantic Oscillation and the Late Maunder Minimum. Meteor Zeit 13:271–289

Zorita E, Gonzalez-Rouco JF, von Storch H, Montavez JP, Valero F (2005) Natural and anthropogenic modes of surface temperature variations in the last thousand years Geophys Res Lett 32: L08707. DOI 10.1029/2004 GLO21563